

# Assessing crop water stress of winter wheat by thermography under different irrigation regimes in North China Plain

Shamaila Zia<sup>1\*</sup>, Du Wenyong<sup>2</sup>, Wolfram Spreer<sup>1</sup>,  
Klaus Spohrer<sup>1</sup>, He Xiongkui<sup>2</sup>, Joachim Müller<sup>1</sup>

(1. Institute of Agricultural Engineering in the Tropics and Subtropics (440e), Garbenstrasse 9, D-70593, Universität Hohenheim, Stuttgart, Germany;

2. College of Science, Centre for Chemicals Application Technology, China Agricultural University, Beijing 100083, China)

**Abstract:** Thermal imaging can be used as an indicator of water stress due to the closure of stomatal aperture. In this paper, we analyzed the robustness and sensitivity of thermography of winter wheat in the North China Plain. The seasonal and diurnal variations of Crop Water Stress Index (CWSI) were evaluated. Five treatments were applied by means of irrigation, with plots receiving (DI) 100% of  $ET_0$ , (D50) 50%, (D16) 16% and (NI) no irrigation. A high correlation was found between stomatal conductance ( $g_s$ ) and CWSI, depending on the phenological stage of the crop with  $R^2 = 0.44$  at pre-heading stage and  $R^2 = 0.77$  at post-heading stage. In addition, a high correlation between yield and CWSI at different growth stages indicates that thermography can predict yield. Hourly measurements of canopy temperature were taken to study the effect of the time of day on image acquisition and it was found that midday was the most appropriate time. These results should assist in designing precision irrigation scheduling for setting the threshold values.

**Keywords:** CWSI, *Triticum aestivum* L., stomatal conductance, canopy temperature, yield

**DOI:** 10.3965/j.ijabe.20120503.007

**Citation:** Zia S, Du W Y, Spreer W, Spohrer K, He X K, Müller J. Assessing crop water stress of winter wheat by thermography under different irrigation regimes in North China Plain. Int J Agric & Biol Eng, 2012; 5(3): —.

## 1 Introduction

Winter wheat is the major crop produced in the North China Plain (NCP), which is also known as the bowl of China, because 50% of the wheat production and 35% of the maize production occurs in this region<sup>[1]</sup>. Only 30% to 50% of annual precipitation overlaps in the wheat-growing season, therefore supplemental irrigation is needed<sup>[2]</sup>. Irrigation water is supplied mainly by

pumping groundwater which is declining very fast<sup>[3]</sup>. Hence, there is a need to improve water use efficiency (WUE) either by applying micro-irrigation strategies<sup>[4,5]</sup> or by determining crop water requirements using plant based approaches such as leaf temperature for plant water stress monitoring.

The use of leaf or canopy temperature as an indicator of plant water status measured by infrared cameras or thermometers is based on the principle that plant stomatal closure takes place during water stress, which results in a decrease of energy dissipation and an increase of canopy temperature<sup>[6,7]</sup>. The magnitude of the rise in canopy temperature among water stressed plants is influenced by successive stress imposition. For example, stress applying at vegetative and anthesis stages raised the canopy temperatures much higher than in plants stressed only once<sup>[8]</sup>. Thermography has several advantages over the commonly used methods for water status detection

**Received date:** 2012-03-31 **Accepted date:** 2012-08-20

**Biographies:** Du Wenyong, PhD, Email: duxli1222@163.com; Wolfram Spreer, PhD, Email: wolfram.spreer@gmx.net; Klaus Spohrer, PhD, Email: ksophrer@uni-hohenheim.de; He Xiongkui, PhD, Professor, Vice-dean of College of Science, Email: xiongkui@cau.edu.cn; Joachim Müller, PhD, Professor, Email: joachim.mueller@uni-hohenheim.de.

\*Corresponding author: Shamaila Zia, PhD student, Tel: +49(0)71145923119; Fax: +4971145923298. Email: shamailazia@gmail.com; shamaila.zia@uni-hohenheim.de.

like soil water content or crop evaporation by climatic parameters. It is a non-invasive, rapid and reliable method<sup>[9,10]</sup>. In addition, thermography allows monitoring large groups of leaves simultaneously, providing an overview of stomatal conductance ( $g_s$ ) variation and dynamics<sup>[11-13]</sup>.

Crop water stress index (CWSI) is the most common index used to quantify water stress based on canopy temperature. It is a helpful tool for quantifying water stress and also can be used for irrigation scheduling. The key to develop the CWSI lies in defining the upper and lower baselines<sup>[14]</sup>. The upper baseline represents water stress in crop when transpiration has ceased, while the lower baseline corresponds to a well-watered crop, which is transpiring at full potential. To determine these baselines, three main environmental variables are needed: plant canopy temperature ( $T_c$ ), air temperature ( $T_a$ ) and vapor pressure deficiency (VPD). Jones<sup>[15]</sup> defined CWSI as introducing reference surfaces for upper and lower baselines. The different approaches to calculate CWSI<sup>[6,14,15]</sup> have been used successfully for water status measurement in different climatic conditions, and crops such as cotton<sup>[16,17]</sup>, wheat<sup>[18]</sup>, maize<sup>[13,19]</sup>, grapevine<sup>[4]</sup> and olive trees<sup>[16]</sup>. Also, they have been correlated with yield<sup>[19-22]</sup> and WUE<sup>[23]</sup>. The objective of this study was to determine the diurnal and seasonal variations of the CWSI and to establish the relationship between CWSI and  $g_s$  at different growth stages of winter wheat. The NCP has a continental monsoon climate with cold, dry winters and hot, humid summers.

## 2 Materials and methods

### 2.1 Experimental site

Field experiments were conducted at Wuqiao experimental station of the China Agricultural University (37°66' N, 116°44' E), located in Wuqiao county, Hebei province, China. The mean annual precipitation in NCP is 560 mm and the rainfall during the experiment was 25 mm measured by a weather station on site. The soil type at the station is a sandy loam, with the field capacity (FC) and wilting point (WP) at different depths (0-90 cm) varying from 33%-37% and 13%-23%, respectively. Winter wheat was sown on 10 October, 2010 and harvested on 15 June, 2011. After winter dormancy, the

crop revived in early March and flowered on 14 May.

### 2.2 Irrigation treatments and experimental design

A pre-sowing irrigation of 75 mm was applied to all treatments. Drip lines with an emitter flow rate of 4 L/h were laid at a spacing of 0.5 m and water was pumped from a deep well near the experimental field. The experiment consisted of five irrigation treatments in two repetitions, having a plot size of 4 m × 3 m. WUE was calculated using the yield (kg) produced per cubic meter of irrigation water. Yield and plant height increased in response to the increased irrigation, while WUE decreased (Table 1). The treatments were designed in such a way that the amount of irrigation water was supplied based on evapotranspiration ( $ET_o$ ). Following are the treatments: 100% water application (D100), 50% water application by closing the alternate drip lines (D50), 16% application when only one out of six drip lines was opened (D16), when no application of water occurred except for rainfall during pre-sowing irrigation (NI), or when implementing typical farmer practice (FP). The FP treatment was irrigated by using a conventional border-irrigation method where the water is pumped onto the field trough through a lay-flat plastic hose and then distributed by gravity. Fertilization, pesticide application and weed control were conducted identically in all the treatments. Grain yield for each treatment was measured at physiological maturity, when the plant turned dull yellow and the kernels became brittle. This was calculated from the number of plants harvested per square meter and the corresponding number of kernels per head and their weight. Plant height was measured two weeks before harvest.

**Table 1 Cumulative amount of water applied, yield, WUE and plant height in all the treatments**

Treatments	Amount of water applied (mm)	Yield ( $t \cdot ha^{-1}$ )	WUE ( $kg \cdot m^{-3}$ )	Plant height (cm)
No irrigation (NI)	-	7.2	-	56.0
D16	89	7.3	8.2	59.4
D50	279	7.6	2.7	60.7
D100	557	8.0	1.4	65.3
Farmer practice (FP)	1800	9.3	0.5	71.2

### 2.3 Soil moisture and stomatal conductance measurements

Volumetric soil water content was measured with a

profile probe “Diviner 2000” (Sentek technologies, Australia). One access tube was installed in every treatment and measurement was made down to a depth of 0.6 m at 0.1 m intervals. Measurements were taken at three-day intervals, before and after irrigation and whenever there was a rainfall occurrence.

Leaf  $g_s$  was measured with a diffusion porometer SC-1 (Decagon devices, USA) at the time of image acquisition. Measurements were taken at three-day intervals on three randomly selected, fully developed, sunlit leaves per plot. Before each measurement, the instrument was calibrated according to the manufacture’s instructions.

**2.4 Image acquisition and analysis**

The crop canopy temperature was measured with an infrared camera (VarioCAM, InfraTec, Germany). The infrared (IR) lens of the camera displays the object scenery on a micro bolometer array with a resolution of  $320 \times 240$  pixels and operates in the 7.5-14  $\mu\text{m}$  wave bands. Pictures were taken between 13:00 and 14:00 when crop water stress and vapour pressure deficit were likely to be maximum, and there was a minimum influence of solar angle on the canopy. Irbis

Professional 3 software was used for the image analysis and corrections were made for emissivity, environment temperature and relative humidity. Emissivity for canopy measurement was set at 0.95 throughout the measurement. Digital and thermal images were merged to differentiate between canopy and background (e.g. soil) during the early stages of crop development. Canopy temperature ( $T_c$ ) was determined as the average temperature along the rows, measured by drawing a free hand area as shown in Figure 1. The histogram shows the frequency distribution of temperature values for the entire thermal image.

CWSI was calculated according to Jones<sup>[15]</sup> as  $(T_c - T_{wet}) / (T_{dry} - T_{wet})$ , where 10 leaves were used as  $T_{wet}$  reference by spraying water on both sides and 10 leaves served as  $T_{dry}$  reference by covering both sides with petroleum jelly (Vaseline) to prevent transpiration. The CWSI was calculated for the entire season, i.e., starting from 6 April that is DOY (Day of year) 95 until 27 May (DOY 147). Diurnal measurements were taken twice: at the pre-heading stage on 30 April (DOY 119) and at the post heading stage on 11 May (DOY 130) with measurements taken at one-hour intervals.

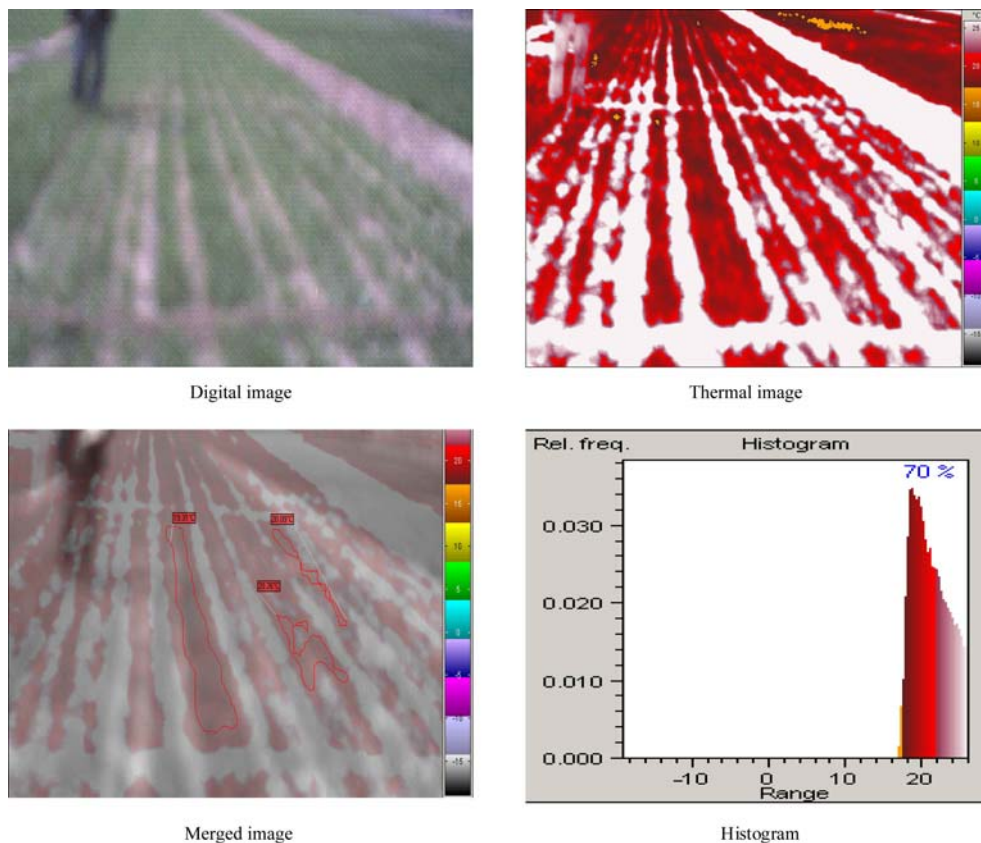


Figure 1 Analysis of thermal image by merging the digital and thermal images

### 2.5 Data analysis and statistics

R statistical program was used in the following analysis: An Analysis of Variance (ANOVA) was performed in order to evaluate the influence of different treatments on canopy temperature, CWSI and  $g_s$  measurements; Linear correlations were calculated for the relationship among canopy temperature, CWSI,  $g_s$ , yield and WUE.

## 3 Results

### 3.1 Weather parameters and soil moisture

The daily average of several weather parameters during the experiment period exhibited great variability. The  $T_a$  and vapour pressure deficit (VPD) increased during the months of May and June (Figure 2). The last days of the experiment were the hottest days with air temperatures exceeding  $28^\circ\text{C}$  and a VPD of about 1.3 kPa. Average wind speed varied between 1 m/s and 4 m/s. A total of 11 rainfall events occurred during the season, supplying 25 mm of water.

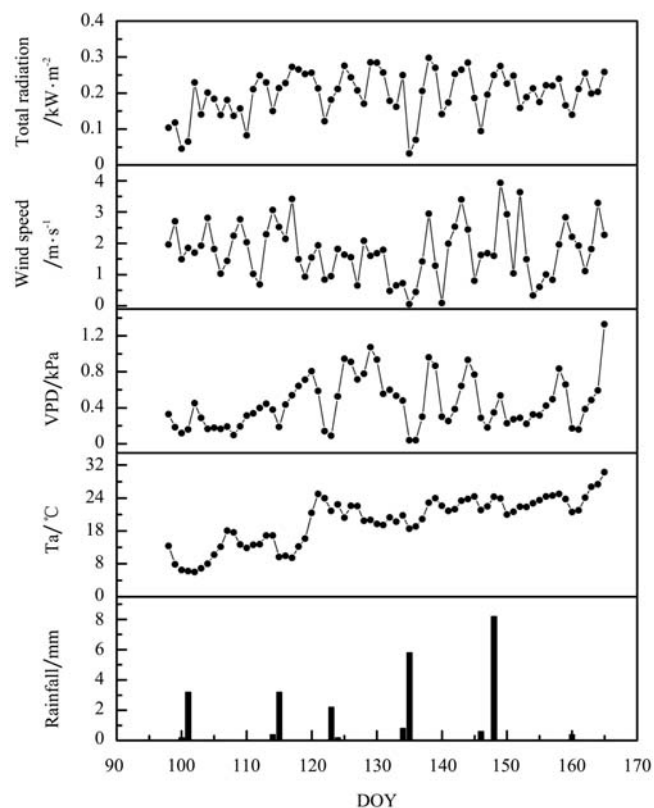


Figure 2 Daily mean values of meteorological parameters on day of year (DOY)

Volumetric soil water content ( $\theta$ ) showed expected trends among treatments (Figure 3). On the farmer's

plot,  $\theta$  was always higher than in the other treatments and never reached the wilting point at any depth. The treatment of NI reached the lowest value of  $\theta$  at 10 cm and was around 12%. At 40 cm depth the variation in  $\theta$  showed expected differences among treatments, with FP having the highest value (32.5%) followed by D100 (22.2%) and D50, D16 and NI, which reached similar values (14%) towards the end of the experiment.

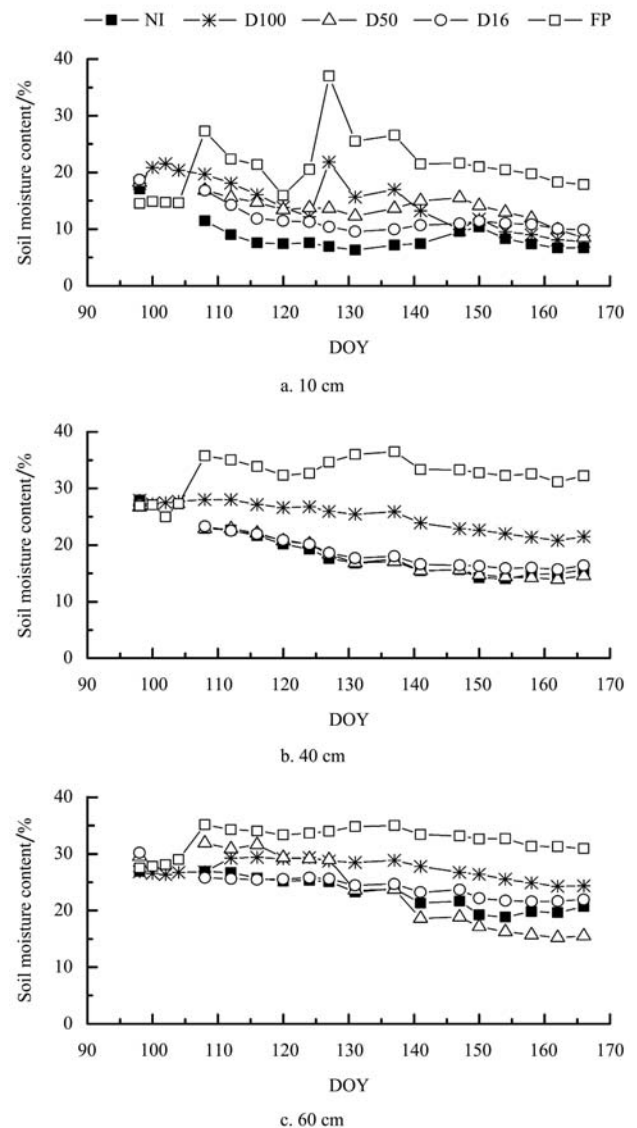


Figure 3 Volumetric soil moisture content in different treatments on day of year (DOY) at three different soil depths

### 3.2 Relationship between soil water content and canopy temperature

Canopy temperature was significantly related to soil moisture at 40 cm depth within each irrigation treatment (Table 2). The intercept indicated the sensitivity level of canopy temperature and soil moisture content as various treatments.

**Table 2 Linear regression relating volumetric soil moisture content (% at 40 cm depth (x-axis) and canopy temperature (°C) (y-axis)**

Treatments	S.E. (intercept)	S.E. (slope)	N	R <sup>2</sup>
NI	35.981	-0.6591	14	0.79***
D16	33.066	-0.5492	11	0.73***
D50	33.755	-0.6033	11	0.73***
D100	29.848	-0.1708	14	0.4*
FP	21.312	0.5782	14	0.53**

Note: N = number of data sets used.

\*\*\*means significant correlation at  $p < 0.001$ ; \*\*means significant correlation at  $p < 0.01$ ; \* means significant correlation at  $p < 0.05$ .

### 3.3 Seasonal variation of CWSI and stomatal conductance

The variations in CWSI are shown in Figure 4 as a function of the different treatments and DOY. Similar trends occurred for each treatment CWSI during the first 10 days of the measurements. Both leaf temperature (data not shown) and CWSI decreased after the irrigation events on DOY 99 and DOY 126. The farmer’s field

was irrigated for the first time on DOY 110 (10 days after the irrigation event of all the other treatments) and the second irrigation event was on DOY 126. The CWSI of the NI treatment was generally higher than the other treatments throughout the experiment. The difference of leaf temperature between NI and FP was observed after the irrigation events on DOY 110 and 126. Similar results were observed for CWSI. The highest CWSI in FP (0.55) and NI (0.8) treatments were observed shortly before harvest, when senescence had started.

Differences became apparent between the two irrigation events and later during the end of the experiment when all the treatments showed an increase in  $T_c$ . Based on the ANOVA test for mean differences, differences of CWSI values between the treatments were significant ( $p < 0.001$ ). The seasonal CWSI for all treatments average all CWSI values measured during the period were 0.33 in FP, 0.43 in D100, 0.56 in D50, 0.61 in D16 and 0.65 in NI.

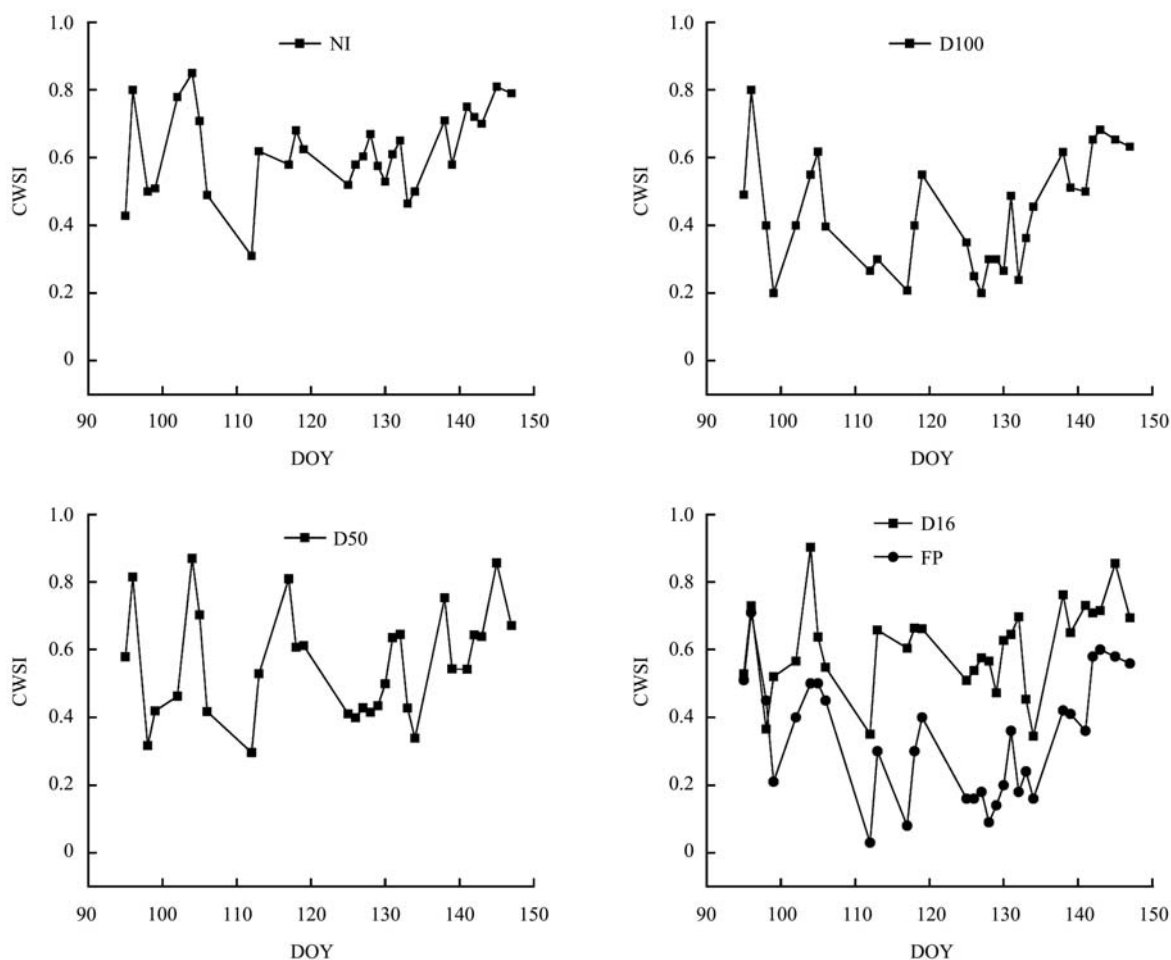


Figure 4 Seasonal variations of crop water stress index (CWSI) for the different treatments on day of year (DOY)

The values of  $g_s$  for NI, D50 and D16 treatments were always below 900  $\text{mmol}/\text{m}^2\cdot\text{s}$ , whereas FP and D100 reached values above 1 300  $\text{mmol}/\text{m}^2\cdot\text{s}$ . The decline in  $g_s$  values and the increase in CWSI (Figure 4) showed an inverse relationship although the effect of treatment did not result in a high statistical significant difference in  $g_s$  values ( $p < 0.1$ ). Higher variations in  $g_s$  values were

observed in the later growth stage (Figure 5). Regardless of growth stage, the NI treatment had the lowest values and the FP had the highest  $g_s$  values throughout the experiment. After the second irrigation event, the differences among NI, D50 and D16 were less visible until end of the experiment. A similar trend can also be seen in the CWSI and  $T_c$  measurements.

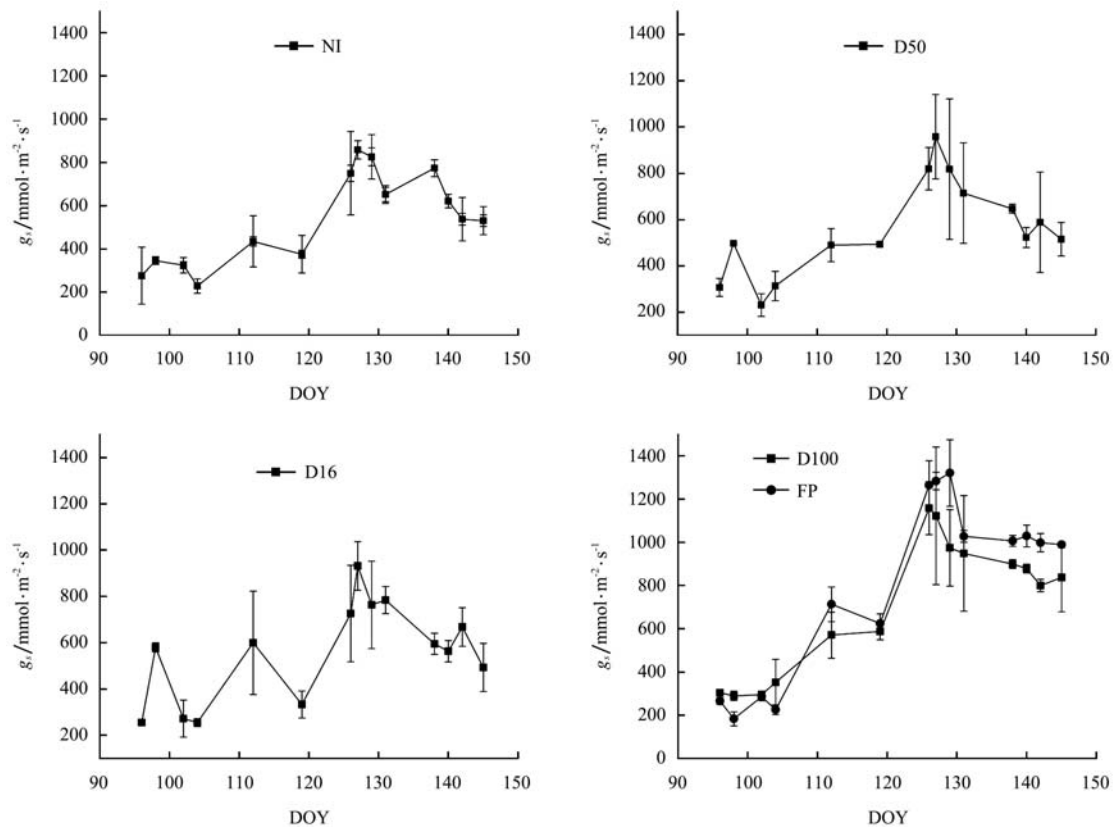


Figure 5 Seasonal variation of stomatal conductance ( $g_s$ ) to water vapour in all treatments on day of year (DOY)

### 3.4 Relationship between CWSI and stomatal conductance

In order to define threshold values for CWSI as an indicator of water stress,  $g_s$  was plotted as a function of CWSI. Results of the experiment showed a linear correlation between CWSI and  $g_s$ , but it depends on the pre- and post-heading phenology. The correlation was higher at the post-heading stage resulting in a  $R^2 = 0.77$  across all the treatments (Figure 6). A fairly good correlation of  $R^2 = 0.44$  was found at the pre-heading stage. During the post-heading stage, both the  $g_s$  and CWSI values were higher than those of the pre-heading stage. The minimum difference in the  $g_s$  values was obtained in the D16 and NI treatments.

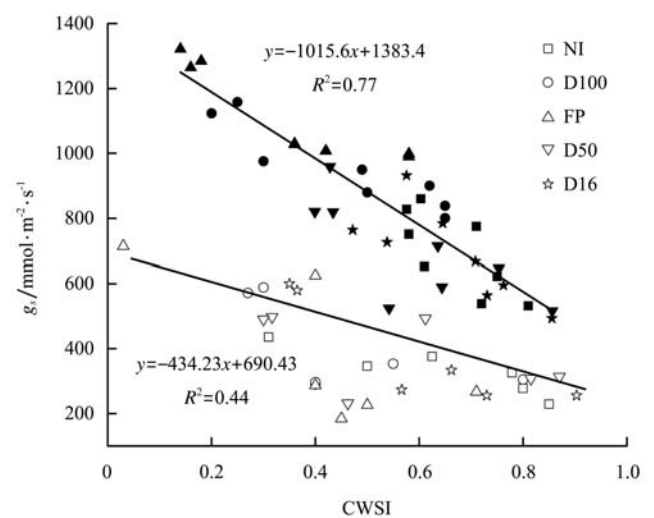


Figure 6 Correlation between CWSI and stomatal conductance ( $g_s$ ) at pre-heading (hollow data points) and post-heading stage (filled data points) for the different treatments

**3.5 Diurnal variations of CWSI**

Meteorological parameters like net radiation ( $R_n$ ), vapour pressure deficit (VPD),  $T_c$ , and the canopy-air temperature difference (the difference between  $T_c$  and  $T_a$  or  $T_c-T_a$ ) on both dates of measurement followed the diurnal trend. The  $T_c-T_a$  was highest at noon (Figures 7

and 8). The  $T_c$  for FP was measured at the post-heading stage only. It can be seen that the difference between the treatments was observed at solar noon and shortly before sunset, whereby the difference between canopy temperature and  $T_a$  of all the treatments decreased.

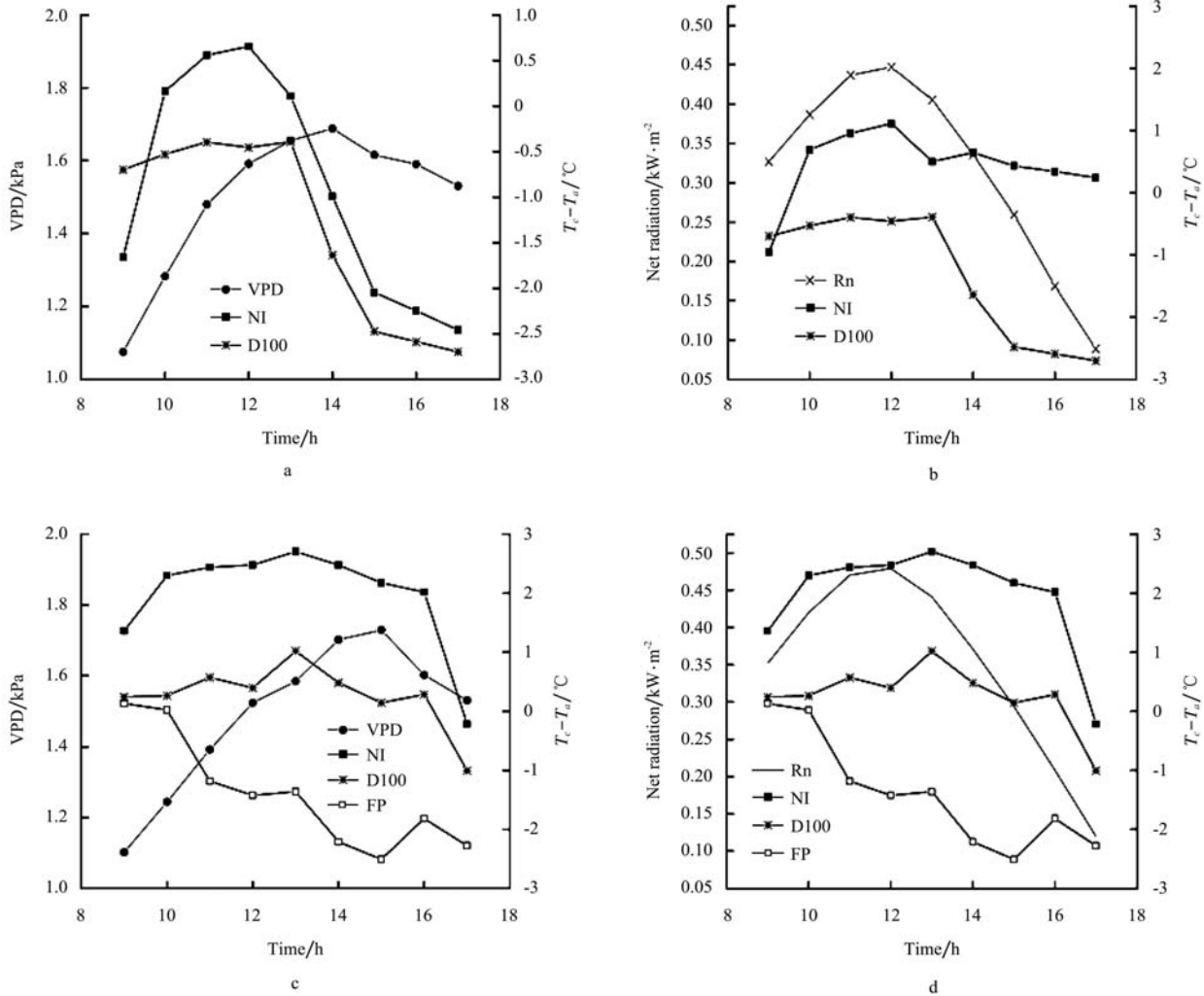
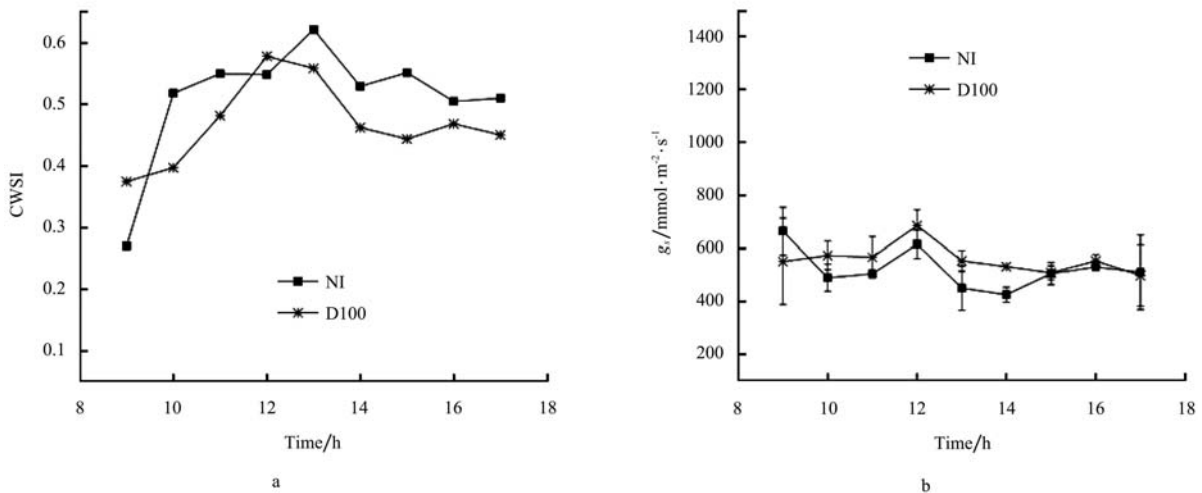


Figure 7 Diurnal course of canopy-air temperature ( $T_c-T_a$ ), net radiation, vapour pressure deficit (VPD), at pre-heading stage (a and b) and post heading stage (c and d) in different treatments



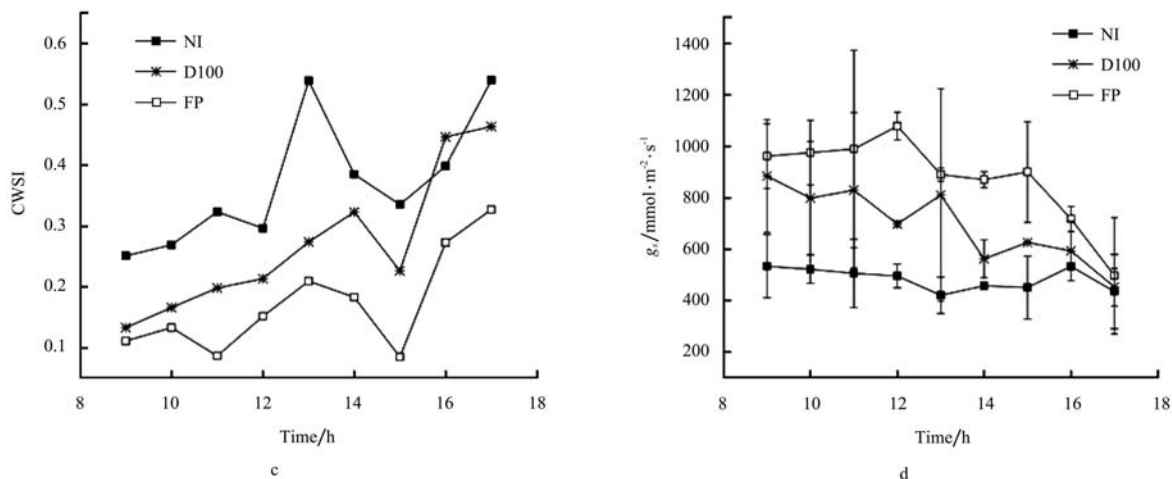


Figure 8 Diurnal course of crop water stress index (CWSI) and stomatal conductance ( $g_s$ ) at the pre-heading stage (a and b) and post heading stage (c and d) in different treatments

The highest CWSI was after solar noon, between 13:00 and 14:00 in all treatments. Variations in  $g_s$  were higher in the morning and late afternoon. A better

correlation between CWSI and  $g_s$  at the post heading stage than that at the pre-heading stage (Figure 9) was observed in all the treatments.

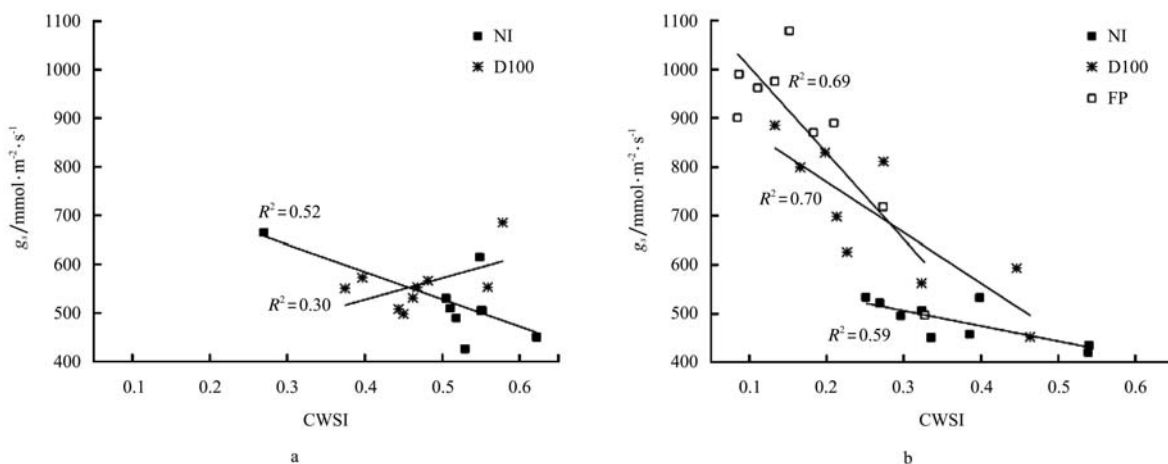


Figure 9 Diurnal correlation between crop water stress index (CWSI) and stomatal conductance ( $g_s$ ) at pre-heading stage (a) and post-heading stage (b) for different treatments

### 3.6 Relationship between yield and CWSI

Yields consistently decreased with increased CWSI within each treatment, with the pre-anthesis response line being distinct from all the others (Figure 10). The values of yield are the average of each treatment, and CWSI is the average value over the pre-heading and post-heading stages, while a CWSI value, 20 days before flowering and immediately after flowering i.e., after seven days were used as pre-anthesis and post-anthesis. As expected, according to CWSI results, the farmer's field had the highest yield of around 9 t/ha. The lowest yield was measured at the NI treatment of around 7 t/ha. There was a significant difference ( $p < 0.05$ ) among yields of every irrigation treatment.

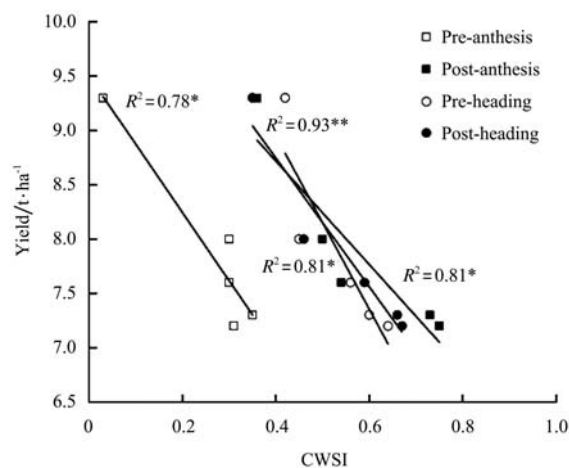


Figure 10 Relationship between CWSI and yield. \*\* Significant correlation at  $p < 0.01$ ; \* Significant correlation at  $p < 0.05$ .

#### 4 Discussion

Though linear correlations were found between  $g_s$  and CWSI, the linear responses differed greatly depending on the phenological stage of the crop. In the present study, we found an  $R^2$  of 0.44 at pre-heading stage and  $R^2$  of 0.77 at the post-heading stage. A similar result was also reported by Yuan et al.<sup>[24]</sup>, who found a linear relationship between leaf water potential and CWSI based on different developmental stages of winter wheat or based on different months. According to Idso<sup>[14]</sup>, the baselines of some crops, including wheat, changes with the growth stage and changes from vegetative to reproductive. A higher canopy diffusion resistance prevails in the post-heading stage than in the pre-heading stage, resulting in a cooler canopy<sup>[25]</sup>. This indicates the importance of considering crop growth parameters like plant height, which affects canopy reflectance and other energy balance components<sup>[26]</sup>. A possible reason for no strong correlation between CWSI and  $g_s$  was found for the entire growing season, which is that the  $g_s$  values varied with the crop development stage, time and days of measurement<sup>[16]</sup>. It has also been reported that thermography can detect variations between treatments even at times when it is not identified by porometry due to the many influencing parameters as stated above, which can result in large variations in the dataset<sup>[27]</sup>. On the other hand, CWSI is solely dependent on the water status of the crop, as a result the overall low correlation between  $g_s$  and leaf temperature might be related to this. Nevertheless, Möller et al.<sup>[28]</sup> reported a high seasonal correlation of about  $R^2 = 0.9$  between  $g_s$  and CWSI on grapevine. However, a close correlation of up to  $R^2 = 0.7$  (Figure 9) was found in our experiments when hourly measurements were taken on a single day, whereby only a negligible variation in the environmental conditions occurred.

The oscillating pattern of seasonal CWSI (Figure 4) indicated that a single measurement is not a true representation of the crop status. Neither negative

values nor values above 1.0 were recorded throughout the experiments, which reinforce the results presented in this study. The use of real leaves instead of black paper or a tensiometer cup as in the previous study<sup>[29]</sup> ensures that the reference surfaces have similar radiative properties as the canopy of interest. A high CWSI was obtained in the beginning, which might be due to the influence of the background soil as the green canopy cover was still small. In general, the CWSI values of FP were 0.33 and D100 was 0.43. This suggests that the winter wheat in NCP should be irrigated when the CWSI reaches a value between 0.3 and 0.4.

The highest  $T_c$  and the lowest  $g_s$  were recorded at solar noon. This indicates that the best time for image acquisition is when the difference between treatments is greatest, although it limits the time interval of image acquisition. This result agrees with previous studies<sup>[13,16]</sup>, where the morning measurements were not as good as those at midday. However, it should be considered that on cloudless days at noon even the well-watered treatments (FP and D100) may close their stomata and might have an increase in leaf temperature<sup>[30]</sup>. Therefore, it is important to determine the timing of measurements for specified conditions and follow it throughout the study<sup>[31]</sup>.

The hourly variation in  $T_c - T_a$  of the NI treatment was positive while it was either zero or negative in FP and D100 treatments. This follows the findings of Jackson et al.<sup>[32]</sup>, where a crop with sufficient water supply will result in  $T_c - T_a$  being either zero or negative, versus  $T_c - T_a$  being positive for a crop with limited water supply. Canopy temperature and CWSI can be used as an indicator of soil water status in winter wheat at a depth of 40 cm. However, measurements at the root depth should also be considered. A good correlation between CWSI and yield at different growth stages implies the use of CWSI as a tool for yield prediction, which is similar to the conclusion of Patel et al.<sup>[7]</sup>. Pre-anthesis and post-anthesis period were considered as the most critical period for yield determination in wheat crop<sup>[33]</sup>.

#### 5 Conclusions

The results of this study showed that the differences in water stress conditions of winter wheat in NCP could be monitored by CWSI by measuring canopy temperature by means of thermal imaging. This method can replace traditional, laborious methods used for identifying the water status of a crop. The seasonal variation of CWSI indicated that its value depends on phenological growth stages of the crop. The temporal variations in canopy temperature and CWSI were highly related to soil water content and yield. The hourly measurement of CWSI and  $g_s$  showed that the best time for image acquisition is between 13:00 and 14:00.

Further investigation should include the effect of leaf angle, which might have a significant influence on the radiation interception. There is still a need to speed up the whole process of image analysis, possibly with further automation to receive the data faster, which can then be used for variable rate applications.

## Acknowledgments

This work was financially supported by Deutsche Forschungsgemeinschaft (DFG)-GRK 1070, Bonn Germany. We are very grateful to the Wuqiao experiment station head and to all the workers of the station, and thankful for their great efforts in supporting the experimental work.

## [References]

- [1] Li J, Inanaga S, Li Z, Eneji A E. Optimizing irrigation scheduling for winter wheat in the North China Plain. *Agriculture Water Management*, 2005; 76: 8-23.
- [2] Zhang J, Sui X, Li B, Su B, Li J, Zhou D. An improved water-use efficiency for winter wheat grown under reduced irrigation. *Field Crop Research*, 1998; 59: 91-98.
- [3] Jinsheng J, Jingjie Y, Changming L. Groundwater regime and calculation of yield response in North China Plain: a case study of Luancheng County in Hebei Province. *Journal of Geographical Science*, 2002; 12: 217-225.
- [4] Grant O M, Tronina L, Jones H G, Chaves M M. Exploring thermal imaging variables for the detection of stress responses in grapevine under different irrigation regimes. *Journal of Experimental Botany*, 2006a; (special edition): 1-11.
- [5] Spreer W, Ongprasert S, Hegele M, Wünsche J N, Müller J. Yield and fruit development in mango (*Mangifera indica* L. cv. Chok Anan) under different irrigation regimes. *Agriculture Water Management*, 2009; 96: 574-584.
- [6] Idso S B, Jackson R D, Pinter J P Jr, Reginato R J, Hatfield J L. Normalizing the stress degree day parameter for environmental variability. *Agricultural Meteorology*, 1981; 24: 45-55.
- [7] Patel N R, Mehta A N, Shekh A M. Canopy temperature and water stress quantification in rainfed pigeonpea (*Cajanus cajan* (L.) Millsp.). *Agricultural and Forest Meteorology*, 2001; 109: 223-232.
- [8] Siddique M R B, Hamid A, Islam M S. Drought stress effects on water relations of wheat. *Botanical Bulletin of Academia Sinica*, 2000; 41: 35-39.
- [9] Cifre J, Bota J, Escalona J M, Medrano H, Flexas J. Physiological tools for irrigation scheduling in grapevine (*Vitis vinifera* L.): An open gate to improve water-use efficiency. *Agriculture, Ecosystem & Environment*, 2005; 106: 159-170.
- [10] Irmak S, Haman D Z, Bastug R. Determination of crop water stress index for irrigation timing and yield estimation of corn. *Agronomy Journal*, 2000; 92: 1221-1227.
- [11] Jones H G. Use of infrared thermometry for estimation of stomatal conductance as a possible aid to irrigation scheduling. *Agricultural and Forest Meteorology*, 1999a; 95: 139-149.
- [12] Jones H G, Stoll M, Santos T, Sousa C, Chaves M M, Grant O M. Use of infrared thermography for monitoring stomatal closure in the field: application to grapevine. *Journal of Experimental Botany*, 2002; 53: 2249-2260.
- [13] Zia S, Spohrer K, Wenyong D, Spreer W, Romano G, He X, et al. Monitoring physiological responses to water stress in two maize varieties by infrared thermography. *International Journal of Agricultural & Biological Engineering*, 2011; 4: 1-9.
- [14] Idso S B. Non-water stressed baselines: a key to measuring and interpreting plant water stress. *Agricultural Meteorology*, 1982; 27: 59-70.
- [15] Jones H G. Use of thermography for quantitative studies of spatial and temporal variation of stomatal conductance over leaf surfaces. *Plant Cell Environment*, 1999b; 22: 1043-1055.
- [16] Bengal A, Agam N, Alchanatis V, Cohen Y, Yermiyahu U, Zipori I, et al. Evaluating water stress in irrigated olives: correlation of soil water status, tree water status, and thermal imagery. *Irrigation Science*, 2009; 27: 367-376.
- [17] Silva B B, Rao T V R. The CWSI variations of a cotton crop in a semi-arid region of Northeast Brazil. *Journal of Arid Environment*, 2005; 62: 649-659.

- [18] Alderfasia A A, Nielsen D C. Use of crop water stress index for monitoring water status and scheduling irrigation in wheat. *Agriculture Water Management*, 2001; 47: 69-75.
- [19] Yazar A, Howell T A, Dusek D A, Copeland K S. Evaluation of crop water stress index for LEPA irrigated corn. *Irrigation Science*, 1999; 18: 171-180.
- [20] Amani I, Fischer R A, Reynolds M P. Canopy temperature depression association with yield of irrigated spring wheat cultivars in a hot climate. *Journal of Agronomy & Crop Science*, 1996; 176: 119-129.
- [21] Chen J, Lin L, Lu G. An index of soil drought intensity and degree: An application on corn and a comparison with CWSI. *Agriculture Water Management*, 2010; 97: 865-871.
- [22] Romano G, Zia S, Spreer W, Sanchez C, Cairns J, Araus J L, Müller J. Use of thermography for high throughput phenotyping of tropical maize adaptation in water stress. *Computer & Electronics in Agriculture*, 2011; 79: 67-74.
- [23] Wang L, Qiu G Y, Zhang X, Chen S. Application of a new method to evaluate crop water stress index. *Irrigation Science*, 2005; 24: 49-54.
- [24] Yuan G, Luo Y, Sun X, Tang D. Evaluation of a crop water stress index for detecting water stress in winter wheat in the North China Plain. *Agriculture Water Management*, 2004; 64: 29-40.
- [25] Tubailish A S, Sammis T W, Lugg D G. Utilization of thermal infrared thermometry for detection of water stress in spring barley. *Agriculture Water Management*, 1986; 12: 75-85.
- [26] Payero J O, Irmak S. Variable upper and lower crop water stress index baselines for corn and soybean. *Irrigation Science*, 2006; 25: 21-32.
- [27] Grant O M, Tronina L, Ramalho J C, Besson C K, Lobo-do-Vale R, Pereira J S, et al. The impact of drought on leaf physiology of *Quercus suber* L. trees: comparison of an extreme drought event with chronic rainfall reduction. *Journal of Experimental Botany*, 2010; 61: 4361-4371.
- [28] Möller M, Alchanatis V, Cohen Y, Meron M, Tsipris J, Naor A, et al. Use of thermal and visible imagery for estimating crop water status of irrigated grapevine. *Journal of Experimental Botany*, 2007; 58: 827-838.
- [29] Zia S, Spohre, K, Merkt N, Wenyong D, He X, Müller J. Non-invasive water status detection in grapevine (*Vitis vinifera* L.) by thermography. *International Journal of Agricultural & Biological Engineering*, 2009; 2: 46-54.
- [30] Grant O M, Chaves M M, Jones H G. Optimizing thermal imaging as a technique for detecting stomatal closure induced by drought stress under greenhouse conditions. *Physiologia Plantarum*, 2006b; 127: 507-518.
- [31] Wanjura D F, Upchurch D R. Canopy temperature characterization of corn and cotton water status. *Transactions of the ASAE*, 2000; 43: 867-875.
- [32] Jackson R D, Reginato R J, Idso S B. Wheat canopy temperature: a practical tool for evaluating water requirements. *Water Resources Research*, 1977; 17: 1133-1138.
- [33] Fischer R A. The importance of grain or kernel number in wheat: A reply to Sinclair and Jamieson. *Field Crops Research*, 2008; 105: 15-21